REVIEW ARTICLE

Multiphoton polymerization of hybrid materials

IOP Publishing Journal of Optics

J. Opt. **12** (2010) 124001 (16pp) doi:10.1088/2040-8978/12/12/124001

REVIEW ARTICLE

Multiphoton polymerization of hybrid materials

Maria Farsari[1], **Maria Vamvakaki**[1,2] **and Boris N Chichkov**[3]

[1] Institute of Electronic Structure and Laser (IESL), Foundation for Research and Technology Hellas (FORTH), N. Plastira 100, GR-71110 Heraklion, Greece
[2] Department of Materials Science and Technology, University of Crete, 71003, Heraklion, Crete, Greece
[3] Laser Zentrum Hannover e.V., Hollerithallee 8, D-30419 Hannover, Germany

Received 11 February 2010, accepted for publication 17 March 2010
Published 11 November 2010
Online at stacks.iop.org/JOpt/12/124001

Abstract
Multiphoton polymerization has been developed as a direct laser writing technique for the preparation of complex 3D structures with resolution beyond the diffraction limit of light. The combination of two or more hybrid materials with different functionalities in the same system has allowed the preparation of structures with advanced properties and functions. Furthermore, the surface functionalization of the 3D structures opens new avenues for their applications in a variety of nanobiotechnological fields.

This paper describes the principles of 2PP and the experimental set-up used for 3D structure fabrication. It also gives an overview of the materials that have been employed in 2PP so far and depicts the perspectives of this technique in the development of new active components.

Keywords: multiphoton polymerization, hybrid materials, 3D structures, direct laser writing, surface functionalization, photonic nanostructures

(Some figures in this article are in colour only in the electronic version)

1. Introduction

Nonlinear optical nanostereolithography based on the two-photon polymerization (2PP) of photosensitive materials is a direct laser writing technique that allows the fabrication of three-dimensional (3D) structures with sub-micron resolution [1–4]. The polymerization is based on two-photon absorption; when the beam of an ultra-fast laser is tightly focused into the volume of a transparent, photosensitive material, the polymerization process can be initiated by nonlinear absorption within the focal volume. By moving the laser focus three-dimensionally through the material, 3D structures can be fabricated. The technique has been implemented with a variety of acrylate and epoxy materials, and several components and devices have been fabricated such as photonic crystal templates [5], mechanical devices [6] and microscopic models [7]. Resolution below 100 nm has been achieved using this technique [8].

The unique capability of 2PP lies in that it allows the fabrication of computer-designed, fully 3D structures with resolution beyond the diffraction limit. No other competing technology offers these advantages. Classic 3D prototyping techniques such as UV laser stereolithography, 3D inkjet printing and laser sintering can also produce fully three-dimensional structures; however, they cannot provide resolution better than a few microns. On the other hand, lithographic techniques with superior resolution, such as e-beam lithography, cannot produce anything more complicated than high-aspect-ratio two-dimensional structures.

The majority of the materials used for 2PP are designed for conventional lithographic applications and there have been examples of both negative and positive photoresists used [9, 1, 3]. In the case of negative photoresists, the two-photon exposure results in the cross-linking of the polymer chains, making the exposed area insoluble to the solvent used to remove the unpolymerized material; so there is a direct writing of the structures in the sample. The opposite happens with positive photoresists; two-photon absorption causes the photoresist polymeric chains to break and become soluble to the development solvent, so the reverse structure

is written in the sample. Negative photopolymers are most commonly used, with the most popular being the UV high-aspect-ratio lithographic photoresist SU-8 and the organic inorganic hybrid ORMOCER®. These materials, while giving excellent structural results, do not provide the functionalization capability required for a lot of applications.

Recently, there have been a series of publications on the development of new, organic/inorganic hybrid sol–gel materials specifically designed for 2PP. Sol–gel technology provides a very powerful tool for the development of photosensitive compounds [10]. These materials benefit from straightforward preparation, modification and processing and, in combination with their high optical quality, post-processing chemical and electrochemical inertness, good mechanical and chemical stability, they can find many applications in photonics, MEMS, microfluidics and biomedicine.

In this paper we summarize the principles of microfabrication by 2PP. We discuss the fundamental principles of two-photon absorption and describe a typical 2PP experimental set-up. Then we concentrate on hybrid materials used for 2PP microfabrication and on recent progress in the functionalization of the surface and the bulk of the 3D fabricated structures, while at the same time discussing applications of the technology.

2. Two-photon polymerization

The basis of two-photon polymerization is the phenomenon of two-photon absorption (TPA). There are two types of two-photon absorption: sequential and simultaneous. In sequential, the absorbing species is excited to a real intermediate state: then a second photon is absorbed. The presence of the intermediate energy state implies that the material absorbs at this specific wavelength; it will therefore be a surface effect and will follow the Beer–Lambert law [11]. The simultaneous absorption, on which the 2PP technique is based, was originally predicted by Göppert-Mayer in 1931 in her doctoral dissertation [12]. It is defined as 'an absorption event caused by the collective action of two or more photons, all of which must be present simultaneously to impart enough energy to drive a transition'. This prediction was not experimentally verified until over 30 years later by Kaiser. Then the invention of the laser permitted the first experimental verification of the TPA when two-photon-excited fluorescence was detected in a europium-doped crystal [13]. In simultaneous absorption, there is no real intermediate energy state, i.e. the material is transparent at that wavelength. Instead, there is a virtual intermediate energy state and two-photon absorption happens only if another photon arrives within the virtual state lifetime [14]. For this to occur high intensities are required, which can only be provided by a tightly focused femtosecond laser beam. This is illustrated in figure 1; as can be seen, the electron transition in this case is caused by two photons of energy $hv/2$ rather than one of energy hv.

Ti:sapphire lasers are widely used for this purpose. They have two main advantages; firstly they have very short pulses, of the order of a few tens of femtoseconds, so they do not cause thermal damage. Secondly their standard wavelength is 800 nm, which is twice the wavelength of polymerization

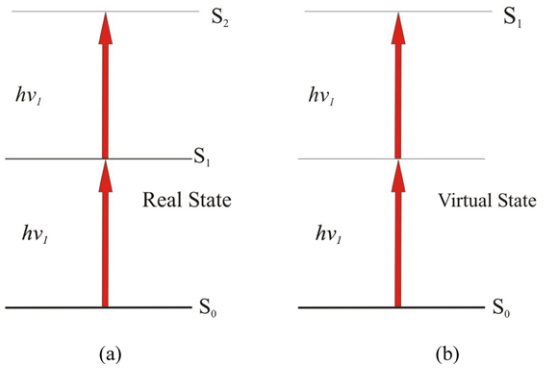

Figure 1. Sequential (a) and simultaneous absorption (b). In the first case the intermediate energy level is an actual energy level, while in the second case it is virtual.

of a wide range of photopolymers. In addition, most photopolymers are transparent at 800 nm, which allows in-volume focusing of the laser beam with minimal scattering.

When the laser is focused tightly into the material, the photoinitiator used to initiate the polymerization will absorb two photons and produce radicals. As the material response is proportional to the square of the intensity, this will only happen at the focal point which, combined with the fact that the two-photon transition rate is very small, will provide very high spatial resolution.

Photopolymerization is a light-induced reaction which converts a liquid or gel monomer into a solid polymer. These reactions require the use of an appropriate photoinitiator which is a light-sensitive molecule that produces an active species upon irradiation with UV, visible or infrared light. The photoinitiators that have been most extensively used so far are divided into two main categories depending on the nature of generated active species (radicals or cations). Conventional photopolymerization initiators generate free radicals upon light irradiation, which initiate a free-radical polymerization process of acrylates or vinyl ethers. Cationic initiators are photo-acid generators that produce cations upon light irradiation and have attracted particular attention since their introduction in the late 1990s. The latter are used for the polymerization of epoxides or vinyl ethers via a cationic polymerization mechanism. The photolysis of cationic photoinitiators has been shown to result in the generation of free radicals allowing the combination of monomers to be polymerized. An effective initiator has a high quantum yield in the generation of the active moieties, high thermal stability and stability in darkness and is highly soluble in the polymerization medium. The most commonly used free-radical photoinitiator is benzophenone and its derivatives. Free-radical polymerizations are chain reactions in which the addition of a monomer molecule to an active chain-end regenerates the active site at the chain-end.

The free-radical photopolymerization mechanism involves at least three different kinds of reactions [15–17]:

- The first step is the initiation during which the free-radical initiator is decomposed with light in the presence of a monomer to form an active species (step (1*a*)).
- In the next step, known as the propagation, the initiator fragment reacts with a monomer molecule to form the

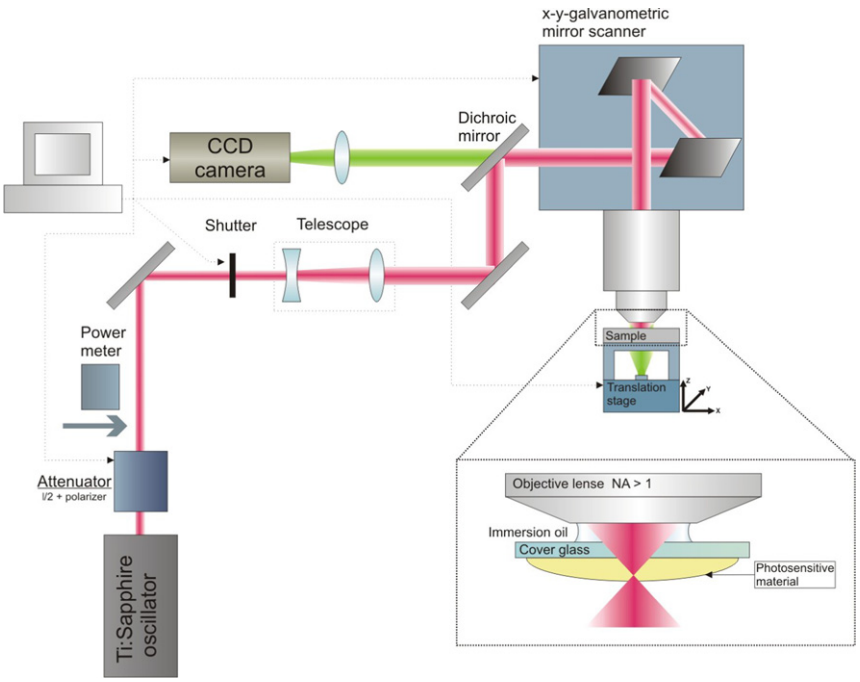

Figure 2. A typical set-up for multiphoton polymerization, consisting of an fs laser, a galvanometric mirror scanner, moving stages, directional and focusing optics, and a monitoring camera.

first active adduct that is capable of being polymerized. Monomers continue to add in the same manner resulting in the formation of macroradicals which are end-active polymers (step (1*b*)).

- The final step is the termination during which the growth center is deactivated and the final polymer molecules are formed. This step normally involves the reaction between two polymers bearing active centers and can proceed by two different mechanisms, combination or disproportionation, leading to the formation of one or two polymer chains, respectively (step (1*c*)):

$$\text{Initiation} \qquad I \xrightarrow{h\nu,h\nu} I^* \longrightarrow R^\bullet \tag{1a}$$

$$\text{Propagation} \qquad R^\bullet + M \longrightarrow RM^\bullet \xrightarrow{M} RMM\cdots \longrightarrow RM_n^\bullet \tag{1b}$$

$$\text{Termination} \qquad RM_n^\bullet + RM_m^\bullet \longrightarrow RM_{n+m}R. \tag{1c}$$

Besides the above, other reactions, such as chain transfer and chain inhibition, often take place and complicate the mechanism of free-radical polymerization.

Photopolymerizations follow the general scheme for any polymerization: however, the use of light, rather than heat, to drive the reaction has certain advantages, such as the elimination of solvent, the high reaction rates at room temperature and the spatial control of the polymerization.

3. The diffraction limit

Theoretically, the highest resolution that can be achieved by a focused laser beam is given by Abbe's diffraction limit [18]:

$$\text{diffraction limit} = \frac{0.5\lambda}{\text{NA}} \tag{2}$$

where λ is the laser wavelength and NA is the numerical aperture of the focusing objective; this has fueled the race for ever decreasing wavelengths, such as electron wavelengths and for alternative, non-light patterning techniques such as atomic force microscopy (AFM) [19–23] and near-field scanning optical microscopy (NSOM) [24–26]. However, these techniques only allow surface and not in-volume patterning. To produce 3D structures with in-volume patterning, and produce photopolymerized voxels smaller than those defined by the diffraction limit, materials with a well-defined photopolymerization threshold need to be used.

As the photoinitiator is excited by the laser process, it produces radicals; these radicals are quenched by oxygen and other quenchers in the system. Quenching is a competing effect to photopolymerization and is usually considered detrimental to the process. In 2PP, however, it can be used to circumvent the diffraction limit and produce structures of very high resolution. This can be done by modifying the light intensity at the focal volume in a manner such that the light-produced radicals exceed the quenchers and initiate polymerization only in a region where exposure energy is larger than the threshold. In this case the diffraction limit becomes just a measure of the focal spot size and it does not really determine the voxel size.

4. Experimental set-up

A typical experimental set-up for the fabrication of three-dimensional microstructures by two-photon polymerization is shown in figure 2. The laser source typically is a Ti:sapphire femtosecond oscillator operating at 800 nm; there are also examples in the literature where an optical parametric oscillator (OPO) is used with a Ti:sapphire laser to reduce the laser wavelength to visible wavelengths [8, 27]. The laser will typically have a pulse length of less than 200 fs and

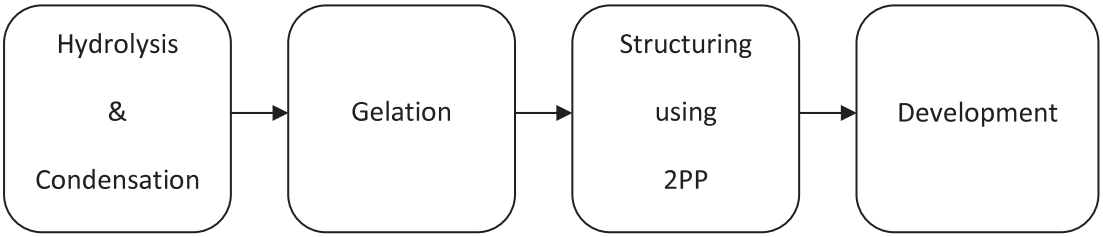

Figure 3. Processing flow of a photosensitive sol–gel.

a repetition rate of 50–80 MHz. The energy required for the polymerization process will depend on the material, the photoinitiator and the focusing, but is usually of the order of a few nanojoules per pulse.

The photopolymerized structure is usually generated in a layer-by-layer format. Each layer is formed either using an x–y galvanometric mirror scanner or x–y piezoelectric stages. The main difference between the two cases being that, in the former case, the structure remains immobile and the structure is generated by the laser beam moving, while in the latter case the x–y stages move the structure and the laser beam remains immobile. Movement on the z axis can be achieved using a piezoelectric or a high resolution linear stage.

To achieve the tight focusing conditions required for two-photon polymerization to occur, a microscope objective needs to be used; when the numerical aperture (NA) of the objective is higher than one, immersion oil is used for index matching. Galvo scanners have to be adapted to accommodate microscope objectives, as usually they are designed to take lenses with long focal lengths.

Beam control can be achieved by either using a fast mechanical shutter or an acousto-optic modulator, while beam intensity control can be achieved using neutral density filters, a variable attenuator or a combination of a polarizer and a waveplate.

For the online monitoring of the photopolymerization process a CCD camera can be mounted behind a dichroic mirror, as shown in figure 2. This is possible as the refractive index of most photopolymers changes during polymerization, so that the illuminated structures become visible during the building process.

When the photosensitive polymer is in a liquid form, in order to avoid liquid movement as the samples moves, the samples are prepared in a sandwich format between two thin glass cover slips; a spacer needs to be used to maintain sample uniformity. When the sample is a solid or a gel, then there is no need for the sandwich format. To avoid the distortion of the focused laser beam by the built structures, they are fabricated layer-by-layer bottom up with the last layer attached to the glass cover slip.

After the completion of the photopolymerization process and in order to remove the unphotopolymerized resin, the samples need to be developed like in any lithographic process. The developer used and the time for development will depend on the material.

5. Materials

The first materials employed in 2PP were acrylic photopolymers and the negative photoresist SU8. Over the last few years, 2PP research has focused on photosensitive sol–gel hybrid materials [28] such as the commercially available ORMOCER® [29–31]. The sol–gel process is based on the phase transformation of a sol of metallic oxide or alkoxide precursors to form a wet gel. A photosensitive sol–gel process usually involves the catalytic hydrolysis of the sol–gel precursor(s) and the polycondensation of the hydrolyzed products and other sol–gel-active components present in the reaction medium to form a macromolecular hybrid network structure. The gel formed is subsequently reacted through photopolymerization to give a product similar to glass.

3D structure fabrication generally involves a four step process, described in figure 3. The first one is hydrolysis and condensation in which precursors or monomers such as metal oxides or metal alkoxides are mixed with water and then undergo hydrolysis and condensation to form a porous interconnected cluster structure. Either an acid such as HCl or a base like NH_3 can be employed as the catalyst:

$$-\overset{|}{\underset{|}{\text{Si}}}\text{–OR} + \text{H–OH} \xrightarrow{\text{hydrolysis}} -\overset{|}{\underset{|}{\text{Si}}}\text{–OH} + \text{R–OH}.$$

The second step is gelation, where the solvent is removed and a gel is formed by heating at low temperature. It is at this stage that solvents are removed and any significant volume loss occurs:

$$-\overset{|}{\underset{|}{\text{Si}}}\text{–OH} + -\overset{|}{\underset{|}{\text{Si}}}\text{–OR} \longrightarrow -\overset{|}{\underset{|}{\text{Si}}}\text{–O–}\overset{|}{\underset{|}{\text{Si}}}- + \text{R–OH}.$$

The third step of the process is the photopolymerization. Because of the presence of double bonds, and provided a photoinitiator is present in the gel, the photoinduced radicals will cause the polymerization of the unsaturated moieties only in the area the radicals are produced. At this step there is no material removal and no volume loss; the only reaction is the addition of the monomers to the active center.

The last step is the development; the sample is immersed in an appropriate solvent and the area of the sample that is not photopolymerized is removed.

6. Silicate hybrid materials

Silicate-based photopolymers have proved to be a very popular choice in microfabrication using multiphoton polymeriza-

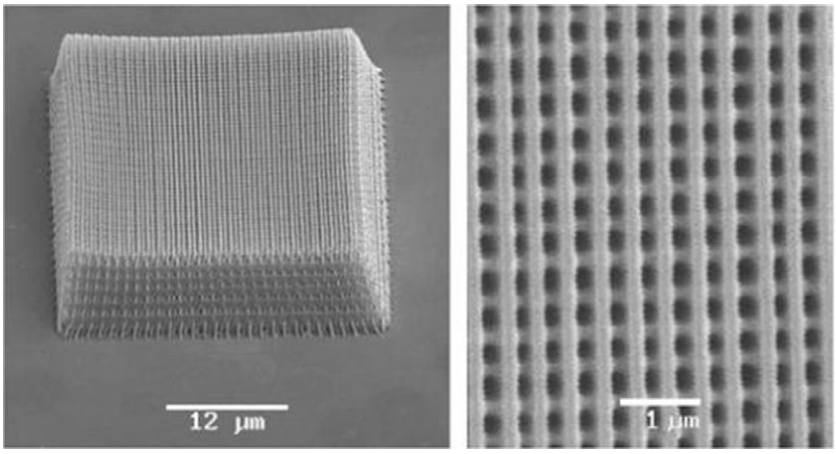

Figure 4. SEM images of ORMOCER® woodpile structures fabricated using 2PP [112].

tion [27, 29, 32, 33]. They combine the properties of silicate glasses such as hardness, chemical and thermal stability, and optical transparency with the laser processing at low temperatures of organic polymers; properties impossible to achieve with just inorganic or polymeric materials. The most widely used hybrid material is the commercially available photopolymer ORMOCER® (ORganically-MOdified-CERamic, MicroResist). This material comprises an inorganic (–Si–O–Si–) backbone which can be functionalized with a range of organic functionalities. ORMOCERs are often used as dental composites [34–37], as electrolytes for lithium batteries [38, 39], as membrane materials for fuel cell applications [40, 41] and in optical interconnect technology [42, 43]. The ORMOCER® widely used in 2PP was firstly developed by Houbertz and its 2PP use was pioneered by the Chichkov group in Laser Zentrum Hannover e.V., Germany. Their first 2PP application was in photonics [30, 29, 44, 45]. Commercially available ORMOCER® was used to fabricate photonic crystal woodpile structures, like the one shown in figure 4 [112].

The good mechanical, optical and processing properties of ORMOCER®, combined with the fact that it is commercially available, made it a very attractive option for the fabrication of photonic crystal structures and devices. A research group at Swinburne University of Technology, Australia used ORMOCER® for the fabrication of waveguide-coupled woodpile structures to investigate superprism phenomena [46, 47], and for the fabrication of diffractive optical elements using 2PP [48]. The same team used ORMOCER® to fabricate woodpile structures and infiltrated them with quantum dots [49]. They showed that the maximum resolution can be increased by post-treating ORMOCER® structures with heat [50]. More recently, a low threshold organic semiconductor distributed feedback laser was fabricated based on a surface grating structured in an ORMOCER® material using two-photon polymerization [51].

Commercially available ORMOCER® is a viscous liquid that does not require any pre-treatment before structuring; this makes its handling straightforward and easy. However, it also has certain drawbacks. As the liquid transforms into a solid during photopolymerization, shrinkage occurs [52], which results in the distortion of the photopolymerized structure and deviation from the original design. This can be corrected using a compensation factor, the effect of which is shown in figure 5 [53, 113].

Another area where three-dimensional microstructures fabricated using ORMOCER® have found application is in biomedical microdevices and medical implants [53–57] due to its biocompatibility and chemical inertness. Figure 6 shows a micro-needle array which can be used in drug delivery devices enabling transdermal delivery of different pharmacological substances. 2PP allows not only the miniaturization of such devices, but also the adoption of more than one needle design in a single array, therefore optimizing the effect of geometry on mechanical and puncturing ability.

7. Composite materials

While ORMOCER® and other silicate-only based hybrid materials have provided the possibility to fabricate high resolution 3D structures with good optical properties, they do not allow the optimization and 'fine tuning' of the material properties for specific applications. The versatile chemistry of sol–gel composites allows the co-polymerization of more than one metal alkoxide; this has been shown to enhance the material's mechanical stability and allows the modification of its optical properties [58–62].

There are several examples of 3D microstructures fabricated using 2PP and acrylate photopolymers doped with metal or metal oxide nanoparticles [63–65]. However, despite the obvious advantages of preparing true composite photosensitive sol–gels, there are very few such examples in 2PP. Bhuian *et al* showed that silicon and zirconium alkoxides can be combined to give a material that can be structured by 2PP [66–68]. Ovsianikov *et al* investigated this material combination further and showed that the silicon alkoxide could be doped up to 30% with a modified zirconium propoxide, allowing the fine tuning of the material's refractive index [69, 70]. They also showed that, under specific fluence conditions, specific material combinations can be structured into complex 3D structures without shrinkage as shown in

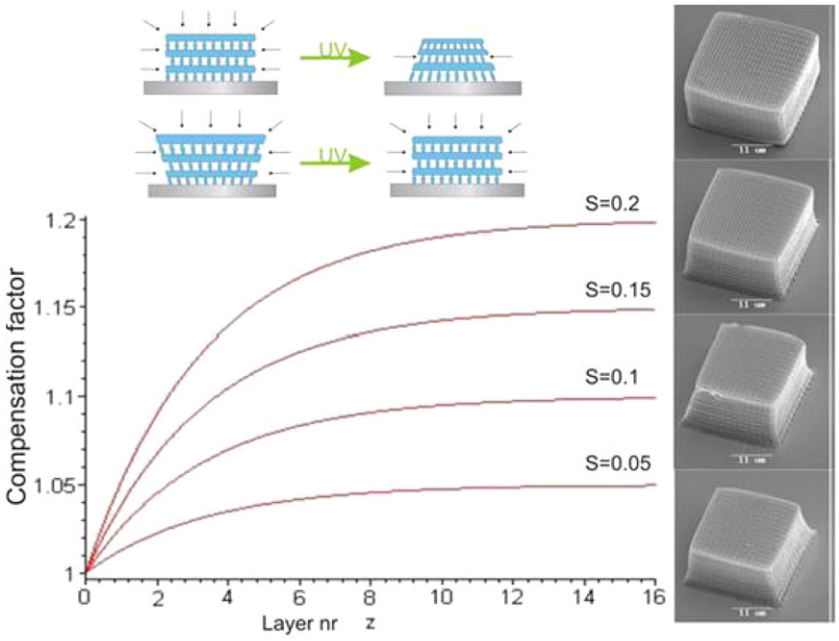

Figure 5. Reduction of shrinkage deformation using a correction factor [113].

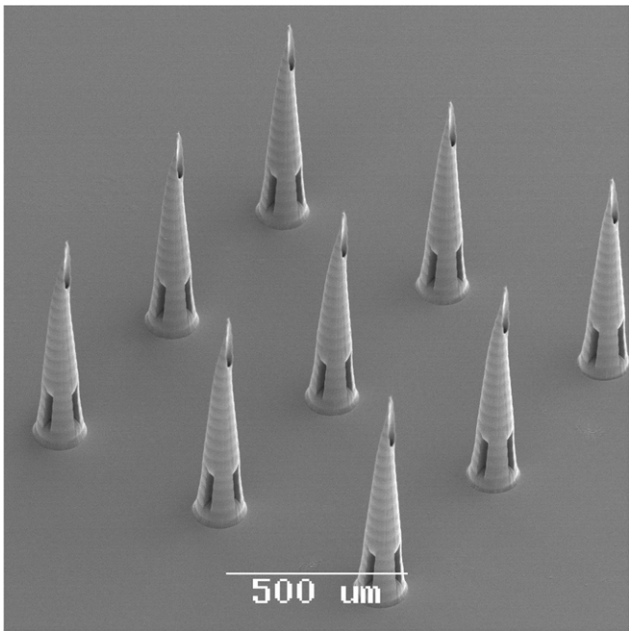

Figure 6. Micro-needles fabricated using 2PP [53].

the SEM images in figure 7 [71]. Further studies have shown that, apart from photonic crystal structures [72], this material can be successfully used for the accurate fabrication of readily assembled microfluidic check-valves (figure 8) [114] and thus is promising for many technological applications. This material combination is now available through IESL-FORTH, Greece under the name SZ2080.[4]

Another material combination investigated recently is silicon and titanium alkoxide [73]. In this case, it was shown that, once the titanium alkoxide content increased above 50%, the non-polymerized material could not be removed and therefore these materials could not be used for two-photon fabrication. However, an 80–20% silicon/titanium combination was used to fabricate good quality woodpile structures with a 200 nm resolution (figure 9).

While there has been limited work in the field on composite sol–gels for 2PP applications, these recent results demonstrate the potential of this material technology. Our team is working on new composite materials which show improved properties and functions, compared to hybrids based solely on silicon alkoxides.

8. Active hybrid materials

The incorporation of an active molecule into a photopolymer is a subject of intense research, as it is desirable to create 3D structures with inherent functionalities. There are several examples of organic photopolymers being doped with active groups; in general, one of the two following approaches is used:

(i) chemical attachment of an active material into a photopolymer;
(ii) a guest–host strategy, where an active material is dispersed into a photopolymer, without the chemical binding of the active materials onto the photopolymerizable structure [74, 75].

Using the first approach, 3D structures containing TiO_2, lasing, conducting and metal-binding materials have been prepared [63–65]. However, none of the structures fabricated to date have been functional. A possible explanation for this is the use of purely organic, acrylate photopolymers as the main structural material. While this kind of material can provide

[4] bmm@iesl.forth.gr

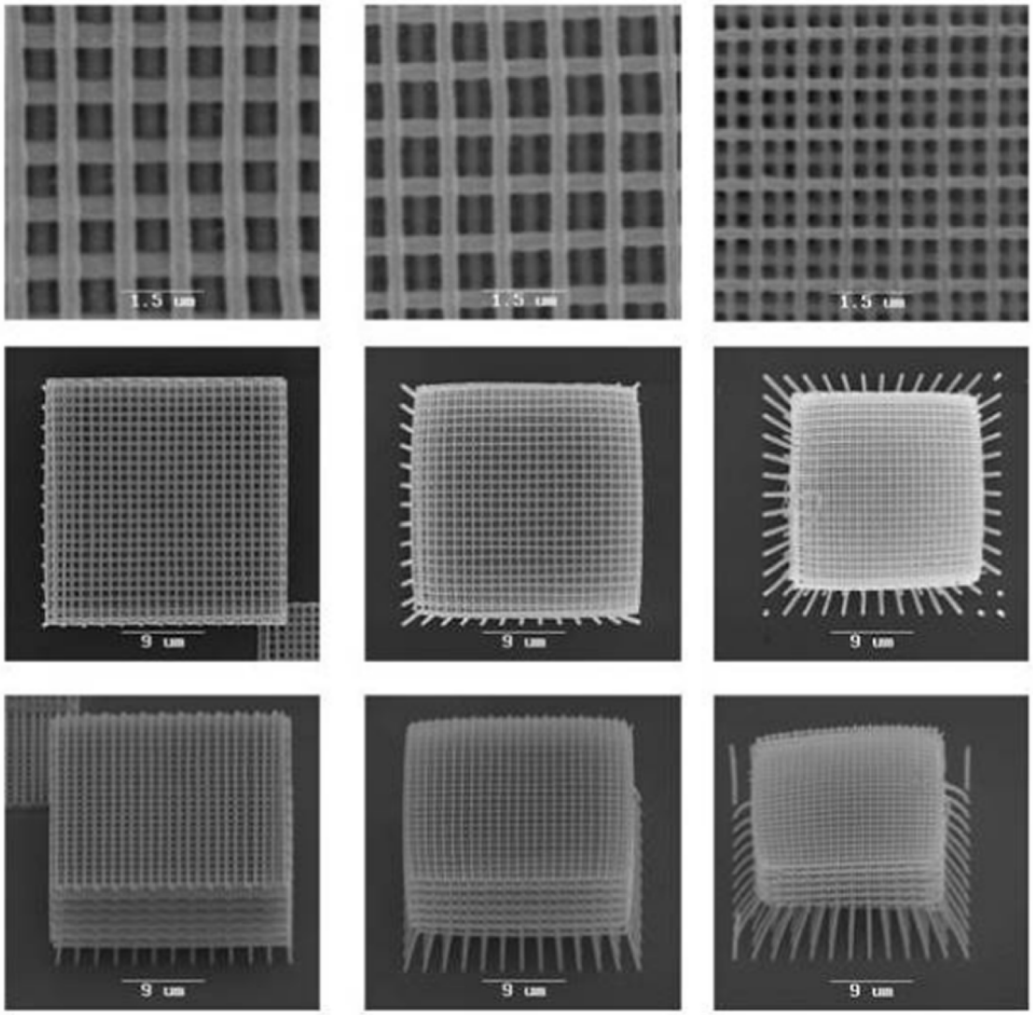

Figure 7. SEM images of representative woodpile structures, showing the effect of shrinkage. From bottom to top: structure side view, top view, and a close-up view of the upper layers are presented. The average laser power used for 2PP reduces from left to right (and the decrease of laser power results in increased material/structure shrinkage and deformation of the supporting columns) [71].

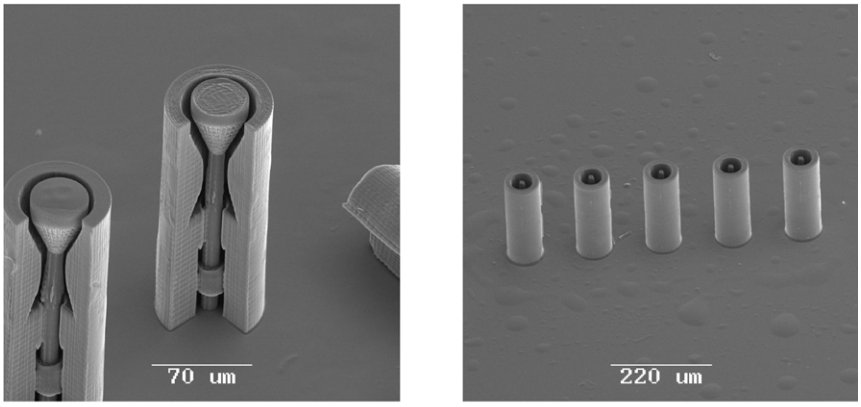

Figure 8. SEM images of (a) three-quarter and (b) whole check-valves [114].

very high resolution at an individual feature level, they cannot be used for the fabrication of structures that have both high resolution and structural integrity.

The second approach has more problems, which are regardless of the material being organic or hybrid. In general, there has been a lot of work involving guest–host hybrid

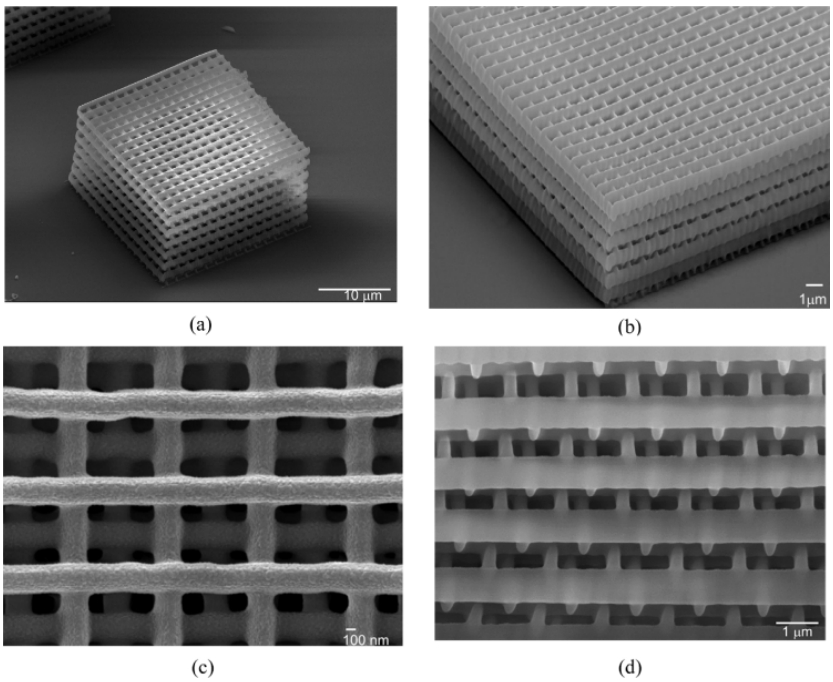

Figure 9. A photonic crystal structure fabricated using a silicon/titanium composite (a), detail of the structure (b), top view (c) and side view (d) [115].

systems, in particular in nonlinear optical (NLO) materials for electro-optic applications. These materials have attracted interest due to their unique properties such as high nonlinearity, low cost, high poling efficiency and stable alignment of nonlinear molecules, leading to high temporal and thermal stability of their nonlinear performance [76–79]. Research to date in this direction has only produced planar electro-optic devices [80–83]. The process followed normally involves the mixing in solution of the polymer or sol–gel with the active medium, the fabrication of the planar device using a film deposition technique such as spin-coating, and finally the polymerization using either light or heat. When it comes to 3D structural fabrication using 2PP, however, there is an extra step needed; the removal of the non-polymerized material by immersion in a development solvent. During this process, a percentage of the dopant molecule is lost. The amount lost depends on the photopolymer, the dopant molecule, the size of the structure's fine features and also the development time—it is possible that, if the structure has very fine features, all dopant is lost. So while it is possible to create structures that demonstrate a proof-of-principle using this approach, the results are too unreliable for any practical applications.

Recently, our team has prepared a nonlinear optically active chromophore hybrid material, which was used to fabricate three-dimensional photonic crystals with stop-gaps in the near-infrared by 2PP microfabrication. The active material used is the well-known and characterized NLO molecule Disperse Red 1 (DR1), which was first reacted with (3-isocyanatopropyl) triethoxysilane to form a functionalized silicon alkoxide precursor (SGDR1). SGDR1 was subsequently mixed with a photosensitive sol, consisting of the polymerizable siloxane precursor methacryloxypropyl trimethoxysilane (MAPTMS) and the photoinitiator Irgacure 369 [116].

Figure 10(a) shows a microscope image of an array of photonic crystals made using this material which have the bright red color of DR1. Figure 10(b) shows an SEM image of a DR1-containing photonic crystal fabricated by the 2PP method while figure 10(c) shows a detail of the same structure. As seen in the figure, SGDR1 can be structured very accurately and without defects. The highest resolution achieved was 250 nm.

The refractive index of the material at 633 nm was determined from an m-line prism coupling experiment, using an He–Ne laser and was found to be $n = 1.497 \pm 0.006$ (10% w/w SGDR1 content) [84, 85]. Since the contrast in refractive index between SGDR1 and air is of the order of 0.5, the fabricated crystals do not possess a complete photonic bandgap. However, in certain directions a photonic stop-gap arises leading to a decrease in transmission. Fourier transform infrared spectroscopy (FTIR) measurements of the transmission spectra of woodpile structures with rod distances between 1.4 and 1.8 μm are shown in figure 11. They indicate the existence of stop-gaps at the expected frequencies, with their central frequency shifting to shorter wavelengths as the rod distance is reduced. It can also be seen that there is noise and a reduction in the transmission at the lower end of the graph; this is because the measurements were carried out at the edge of the detection limit of the FTIR detector. Previous studies have shown that DR1 sol–gel co-polymers exhibit second-order nonlinearity, with $d_{33} = 30$–55 pm V^{-1} at 1300 nm, depending on the DR1 content [86]. To manifest this nonlinearity, the symmetry in the material needs to be removed; this can be done by corona poling the samples at elevated temperatures. Once corona poled, the samples have been reported to exhibit excellent optical as well as mechanical stability. On the other hand, it would be easier to use materials

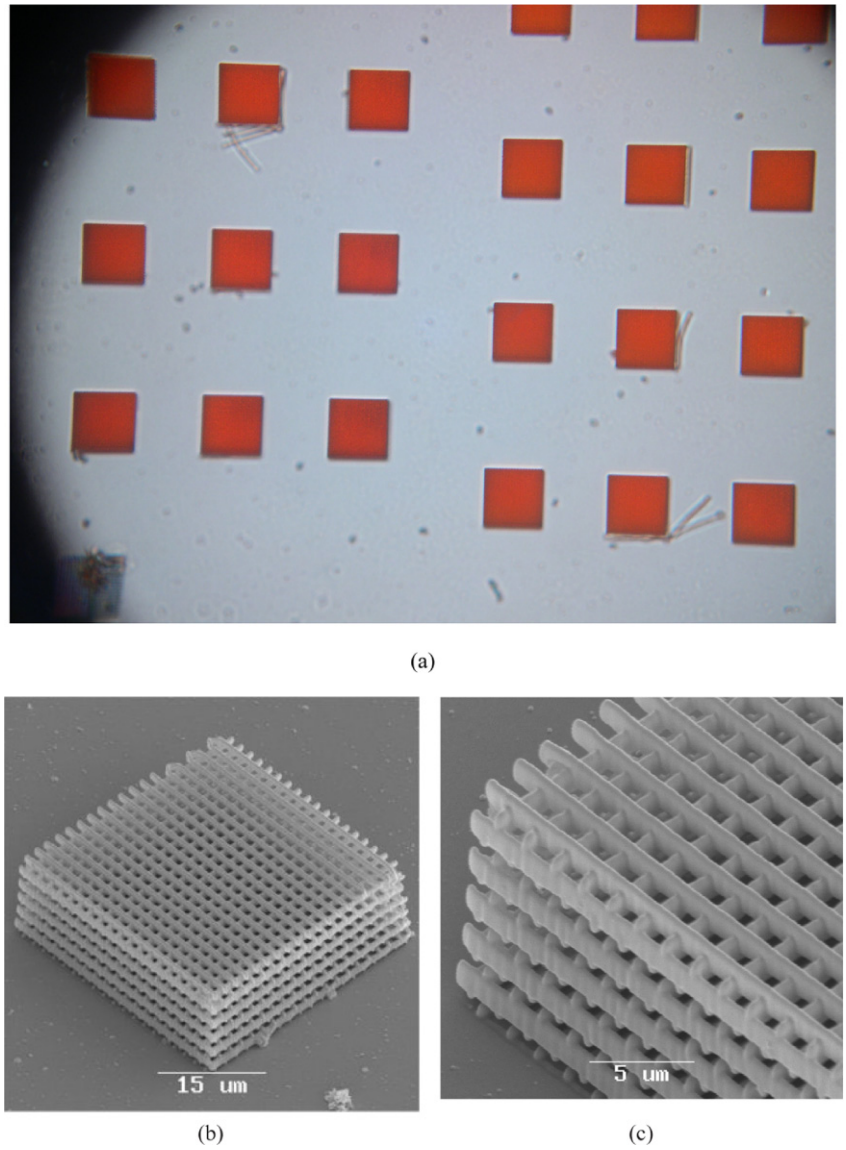

(a)

(b) (c)

Figure 10. Optical microscope image of an array of photonic crystals made by an SGDR1 composite (a), SEM image of a DR1-containing woodpile structure (b) and a detail of the structure shown in (b) and (c) [116].

with third-order nonlinearity, which do not require non-centrosymmetry. They, however, raise another complication; as the removal of centrosymmetry in not needed, it is possible to generate third harmonic light while structuring the material. As an 800 nm laser is normally used for 2PP, the third harmonic produced would be in the UV, where the photoinitiator absorbs; it is therefore possible that, instead of a two-photon polymerization process, a one-photon polymerization might occur by the third harmonic light, which would result in the lose of the polymerization localization and the high resolution obtained by 2PP. In general, this will not happen if the material has a component, other than the photoinitiator, that will absorb in the UV region. In this case, the third harmonic light will be absorbed by the chromophore, instead of the photoinitiator, and the one-photon polymerization will cease. One such example is, in fact, the DR1 composite described earlier; this material possesses a third-order nonlinearity and generates third harmonic: however, it does not polymerize under UV light and can thus be structured accurately using 2PP.

9. Surface functionalization

While there has been a lot of active research targeting the development of novel photostructurable materials for 2PP fabrication, there has also been a lot of activity in the field of the surface functionalization of the 3D structures. The main application areas targeted here are optical-wavelength metamaterials, where there is a requirement for sub-wavelength, metal-covered structures and biosensors, where the structures need to be functionalized with biomolecules.

In the case of metamaterials, where very high resolution is required, most research to date has been carried out using the photoresist SU8. To this end, two completely different approaches have been developed; in the first, the structure

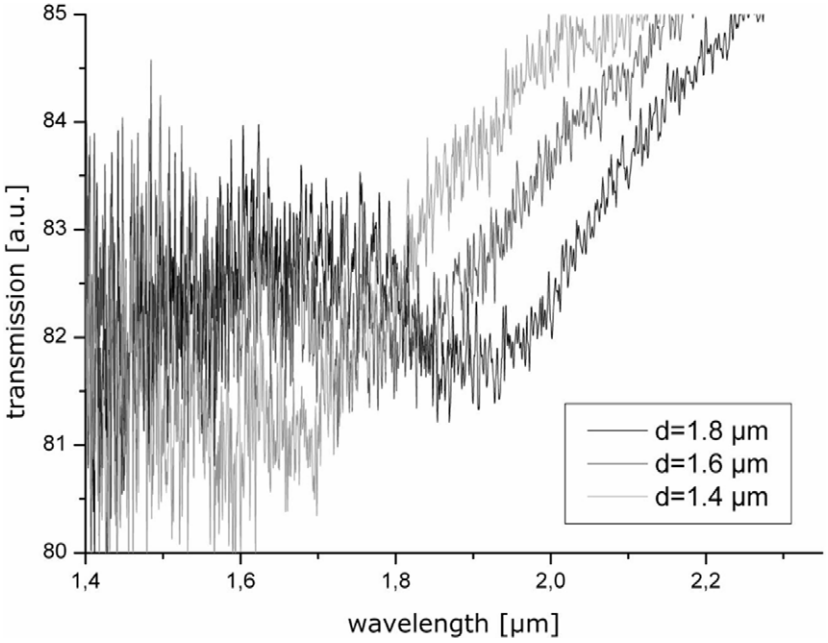

Figure 11. FTIR measurements of the transmission spectra.

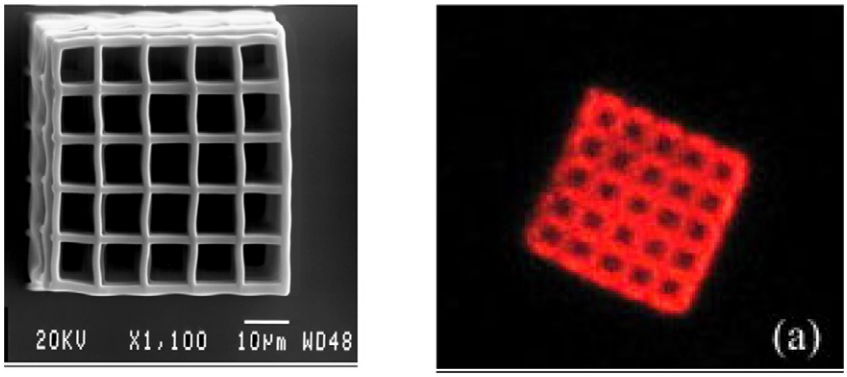

Figure 12. SEM (a) and fluorescence image (b) of a 3D structure with photolytically attached biotin and streptavidin. The 3D component fluoresces very strongly when exposed to green light.

surface is activated using chemical etching, followed by metal deposition by electroless plating [87, 88]. In the second case, complementary, chemical vapor deposition is used to cover the surface of the structures with metal [89]. Both techniques are not dependent on the material used and could be used with hybrid materials. To date, however, there is no published work in this field.

When it comes to functionalizing the surface of 3D structures with biomolecules, we have shown that it is possible to functionalize the surface of 3D ORMOCER® structures with photosensitive biotin [90, 91]. Photochemical activation of light-sensitive molecules is a very versatile method and several materials have been used to create patterned surfaces [92, 93]. The use of photoactive biotin derivatives to create patterned surfaces is a very attractive technique for the following reasons; first, it allows the exploitation of a strong non-covalent biological interaction between biotin and the glycoprotein streptavidin [94]; second, the tetrameric nature of streptavidin allows for further binding of biotinylated ligands and therefore the creation of larger assemblies of molecules onto the surface of the sample [95, 96].

In our work, 3D structures were made using ORMOCER®. Biotin was subsequently immobilized on the surface of these structures by excimer laser photolysis of photobiotin; the latter was further derivatized by fluorescently labeled streptavidin, which allowed the visualization of the distribution of the streptavidin by fluorescence microscopy.

Figure 12(a) shows the SEM image of a structure built employing multiphoton polymerization. The structure consisted of five step-in squares, which served the purpose of building a robust support structure and four vertical and horizontal lines, which served as dividers. Figure 12(b) depicts the image of a similar component after treatment with photobiotin/streptavidin using a fluorescent microscope. It can

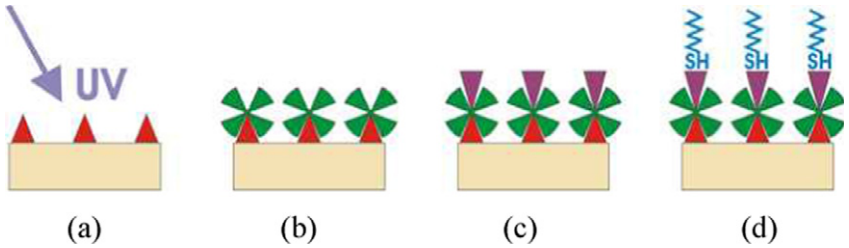

Figure 13. Functionalization of ORMOCER® for peptide fibril growth. A thin layer of photobiotin (red triangles) is deposited on the ORMOCER® surface and exposed to UV light (a) before being further functionalized with avidin (green crosses) (b) and iodoacetamide-functionalized biotin (purple triangles) (c). The final step is the attachment of the cysteine-containing peptide through the SH-iodoacetamide reaction (d).

be seen that the 3D component fluoresces very strongly when excited with green radiation. This fluorescence is restricted solely on the component and on the glass substrate. As ORMOCER® and photobiotin do not fluoresce in the green, it is safe to conclude that streptavidin is responsible for the observed fluorescence. This was further confirmed using SAW sensor technology [90].

This method for fabricating 3D biopolymer-functionalized structures is straightforward and can provide the basis for developing a wide variety of structures by exploiting the binding capabilities of the biotin–streptavidin system. In a subsequent study, we investigated the functionalization of the 3D structures using amyloid peptide fibers [97]. In general, fibrous nanostructured objects are promising for integration in future generations of micro- and nanodevices with carbon and inorganic nanotubes being most commonly investigated due to possible related industrial applications [98]. Nanofibers and nanotubes of biological origin offer the advantage of synthesis under mild, physiological conditions; DNA fibers are the first nanoscale bio-materials that were demonstrated to function as building blocks in nanotechnology set-ups [99, 100]. Another class of fibers are protein-based, such as natural fibrous proteins (silk fibroins, spider silks and viral fibers) and fibers formed through the self-assembly of proteins and peptides [101, 102]. The latter include the so-called amyloid fibers that form following protein misfolding and misassembly events and result in pathological states associated with human diseases [103]. These families of proteins and peptides share common features, such as controlled assembly from repetitive building blocks, and exceptional resistance to extreme conditions such as high and low temperature, detergents and denaturants. This resistance to extreme conditions makes them attractive candidates for applications in nanotechnological components, since it allows their interfacing with the world of 'hard materials'. Furthermore, the possibility of introducing site-specific changes at the sequence level offers the major advantage of tailor-made modifications.

In our work we used biotin-functionalized 3D structures, and exploited thiol chemistry and self-assembly of peptide fibrils. These structures consisted of ORMOCER®. First, biotin was immobilized on them (figure 13(a)) and they were next incubated with avidin (figure 13(b)) and subsequently with iodoacetamide-functionalized biotin, *N*-(biotinoyl)-*N*′-(iodoacetyl) ethylenediamine, (figure 13(c)). Finally, the functionalized 3D structures were immersed in an aqueous solution of peptides that contained a cysteine residue. The peptide solutions were 'aged' so that self-assembled fibrils were already formed in solution. The self-assembly of the peptide fibrils into bridges on the structures was initiated through the controlled evaporation of water (figure 13(d)). However, in order for this to occur between two specific positions, a seed, or 'anchoring point', was required. This was provided by the covalent bond formation between the iodoacetamide group in the biotin derivative and the thiol group of the cysteine. The requirement for the 'seeding', and therefore the selectivity of the technique, was demonstrated with the use of peptides that did not contain cysteine. In this case, self-assembled peptide fibrils were formed in solution, but there was no peptide fibril attachment on the functionalized structures.

Peptide fibrils were visualized by SEM or using the well-established diagnostic test of fluorescence emission of the dye Thioflavin T that binds specifically to amyloid fibrils and gives blue fluorescence when excited at 440 nm. A thioflavin fluorescence image and an SEM image of the directed 3D assembly of the peptide fibrils is shown in figures 14(a) and (b), respectively. In this case, a series of 3D columns was fabricated and subsequently functionalized as described earlier. The peptide bridges appeared to form over the shortest distance, as can be seen in the SEM image of figure 4(a). The length and the diameter of the peptide fibrils depended on the design of the 3D structures, i.e. the distance between them and the diameter of the fibril support (figures 15(b) and (c)). Once the fibril bridges were formed, they remained at their position even when the sample was immersed in water for as long as 24 h.

The above method is based on biotin–avidin and thiol chemistry. Thiol-functionalized biomolecules can be easily produced in a laboratory scale and are even commercially available, so this method should be applicable not only to peptides, but to other self-assembling biomolecules as well. Amine-reactive biotinylation reagents are also commercially available and can be used as an alternative to the thiol-reactive biotinylation reagent used in this work. Furthermore, as photobiotin can be easily attached to many different materials, this technique is suitable for a variety of applications and materials.

Peptide fibrils, nanotubes and nano-assemblies have already been employed in biosensors [104–106], and could

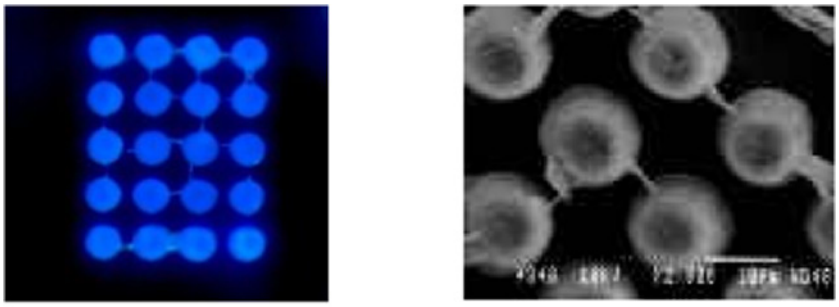

(a) (b)

Figure 14. (a) Thioflavin fluorescence image and (b) SEM image of a 3D column array, with peptide bridges self-assembled between the columns.

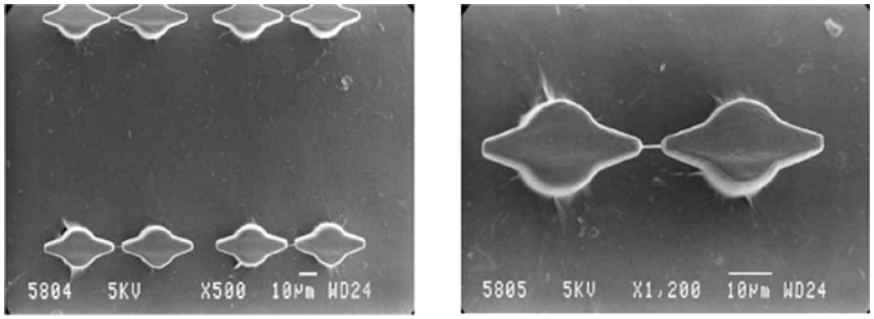

(a) (b)

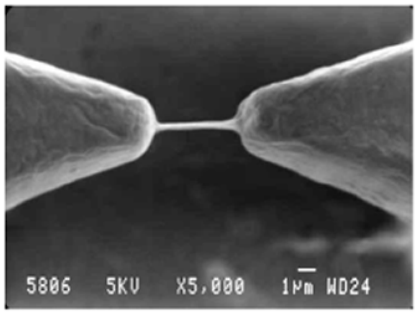

(c)

Figure 15. (a) SEM image of a series of 3D ORMOCER® columns, with peptide fibril bridges self-assembled between them. (b) One pair of 3D ORMOCER® columns, with peptide fibril bridges self-assembled between them. (c) Detail of the self-assembled fiber bridge.

potentially prove more useful, as their chemistry can be easily tailored to provide certain functionality such as specific biomolecule recognition. In addition, their fabrication is considerably less costly and does not involve extreme conditions such as high temperature or vacuum, and the use of certain chemicals.

In molecular electronics, the use of peptide fibrils as templates for the growth of inorganic materials, such as metals (silver, gold and platinum), ferromagnetic metals (cobalt and nickel) and semiconducting materials is of particular interest [107, 108]. In nature, the organization of inorganic matter is often precisely controlled through templating mechanisms mediated by fibrous proteins. Well-known examples include the epitaxial growth of nacre in oysters and silicate spicules in sponges. In a pioneering work, metal and semiconductor-binding peptides were displayed at the surface of filamentous bacteriophages and were used for the fabrication of conductive and semiconductive nanowires [109]. A natural continuation of the work presented here will be the use of mineralized peptide fibers, since cysteine is a metal-binding amino acid. The use of peptide building blocks functionalized with semiconductor-binding sequences can also be foreseen. This will enable the direct self-assembly of nanoscale electronic circuits and devices.

Another field in which our methodology would be particularly applicable is tissue engineering. Peptide networks are already investigated as cell supports in the form of injectable hydrogels [110, 111]. A combination of larger scaffolds with well-defined biodegradable peptide supports in a 'scaffold on scaffold' format could possibly be used as a support for the direct growth of several cell types into ordered arrays of functional biological units.

10. Conclusions

Multiphoton polymerization allows the fabrication of fully three-dimensional structures with sub-diffraction limit resolution. While up to now most research efforts have involved the use of acrylate materials or SU8, the potential of photostructurable hybrid materials for 2PP fabrication has started to emerge. Their mechanical and chemical stability, combined with their superior 2PP structurability and functionalization potential, renders them ideal candidates for a wide range of applications including photonics, metamaterials and biomedical implants.

References

[1] Sun H-B and Kawata S 2004 *NMR. 3D Analysis. Photopolymerization* ed N Fatkullin (Berlin: Springer) pp 169–273

[2] LaFratta C N, Fourkas J T, Baldacchini T and Farrer R A 2007 Multiphoton fabrication *Angew. Chem. Int. Edn* **46** 6238–58

[3] Juodkazis S, Mizeikis V and Misawa H 2009 Three-dimensional microfabrication of materials by femtosecond lasers for photonics applications *J. Appl. Phys.* **106** 051101

[4] Farsari M and Chichkov B N 2009 Two-photon fabrication *Nat. Photon.* **3** 450–2

[5] Deubel M, Wegener M, Linden S, von Freymann G and John S 2006 3D–2D–3D photonic crystal heterostructures fabricated by direct laser writing *Opt. Lett.* **31** 805–7

[6] Galajda P and Ormos P 2001 Complex micromachines produced and driven by light *Appl. Phys. Lett.* **78** 249–51

[7] Park S H, Yang D Y and Lee K S 2009 Two-photon stereolithography for realizing ultraprecise three-dimensional nano/microdevices *Laser Photon. Rev.* **3** 1–11

[8] Haske W, Chen V W, Hales J M, Dong W T, Barlow S, Marder S R and Perry J W 2007 65 nm feature sizes using visible wavelength 3D multiphoton lithography *Opt. Express* **15** 3426–36

[9] Gansel J K, Thiel M, Rill M S, Decker M, Bade K, Saile V, von Freymann G, Linden S and Wegener M 2009 Gold helix photonic metamaterial as broadband circular polarizer *Science* **325** 1513–5

[10] Livage J and Sanchez C 1992 Sol–gel chemistry *J. Non-Cryst. Solids* **145** 11–9

[11] Jacobs P F 1992 *Rapid Prototyping and Manufacturing: Fundamentals of Stereolithography* (Dearborn, MI: Society of Manufacturing Engineers)

[12] Göppert-Mayer M 1931 Über Elementarakte mit zwei Quantensprüngen *Ann. Phys.* **401** 273–94

[13] Kaiser W and Garrett C G B 1961 Two-photon excitation in CaF_2:Eu^{2+} *Phys. Rev. Lett.* **7** 229–32

[14] Varadan V K, Jiang X and Varadan V V 2001 *Microstereolithography and Other Fabrication Techniques for 3D MEMS* (Chichester: Wiley)

[15] Stevens M P 1999 *Polymer Chemistry: An Introduction* (New York: Oxford University Press)

[16] Allcock H R, Lampe F W and Mark J E 2003 *Contemporary Polymer Chemistry* (Upper-Saddle River, NJ: Pearson–Prentice-Hall)

[17] Hiemenz P C and Lodge T P 2007 *Polymer Chemistry* (New York: CRC Press)

[18] Born M and Wolf E 1999 *Principles of Optics* (Cambridge: Cambridge University Press)

[19] Sauer B B, McLean R S and Thomas R R 1998 Tapping mode AFM studies of nano-phases on fluorine-containing polyester coatings and octadecyltrichlorosilane monolayers *Langmuir* **14** 3045–51

[20] Agarwal G, Naik R R and Stone M O 2003 Immobilization of histidine-tagged proteins on nickel by electrochemical dip pen nanolithography *J. Am. Chem. Soc.* **125** 7408–12

[21] Amro N A, Xu S and Liu G Y 2000 Patterning surfaces using tip-directed displacement and self-assembly *Langmuir* **16** 3006–9

[22] Garno J C, Yang Y Y, Amro N A, Cruchon-Dupeyrat S, Chen S W and Liu G Y 2003 Precise positioning of nanoparticles on surfaces using scanning probe lithography *Nano Lett.* **3** 389–95

[23] Liang J and Scoles G 2007 Nanografting of alkanethiols by tapping mode atomic force microscopy *Langmuir* **23** 6142–7

[24] Betzig E and Trautman J K 1992 Near-field optics-microscopy, spectroscopy, and surface modification beyond the diffraction limit *Science* **257** 189–95

[25] Heinzelmann H and Pohl D W 1994 Scanning near-field optical microscopy *Appl. Phys.* A **59** 89–101

[26] Samori P 2004 Scanning probe microscopies beyond imaging *J. Mater. Chem.* **14** 1353–66

[27] Straub M, Nguyen L H, Fazlic A and Gu M 2004 Complex-shaped three-dimensional microstructures and photonic crystals generated in a polysiloxane polymer by two-photon microstereolithography *Opt. Mater.* **27** 359–64

[28] Penard A L, Gacoin T and Boilot J P 2007 Functionalized sol–gel coatings for optical applications *Acc. Chem. Res.* **40** 895–902

[29] Houbertz R, Frohlich L, Popall M, Streppel U, Dannberg P, Brauer A, Serbin J and Chichkov B N 2003 Inorganic–organic hybrid polymers for information technology: from planar technology to 3D nanostructures *Adv. Eng. Mater.* **5** 551–5

[30] Houbertz R *et al* 2003 Inorganic–organic hybrid materials for application in optical devices *Thin Solid Films* **442** 194–200

[31] Houbertz R, Declerck P, Passinger S, Ovsianikov A, Serbin J and Chichkov B N 2007 Investigations on the generation of photonic crystals using two-photon polymerization (2PP) of inorganic–organic hybrid polymers with ultra-short laser pulses *Phys. Status Solidi* a **204** 3662–75

[32] Farsari M, Filippidis G and Fotakis C 2005 Fabrication of three-dimensional structures by three-photon polymerization *Opt. Lett.* **30** 3180–2

[33] Jun Y, Nagpal P and Norris D J 2008 Thermally stable organic–inorganic hybrid photoresists for fabrication of photonic band gap structures with direct laser writing *Adv. Mater.* **20** 606–10

[34] Manhart J, Kunzelmann K H, Chen H Y and Hickel R 2000 Mechanical properties of new composite restorative materials *J. Biomed. Mater. Res.* **53** 353–61

[35] Rosin M, Urban A D, Gartner C, Bernhardt O, Splieth C and Meyer G 2002 Polymerization shrinkage-strain and microleakage in dentin-bordered cavities of chemically and light-cured restorative materials *Dent. Mater.* **18** 521–8

[36] Hurmuzlu F, Kiremitci A, Serper A, Altundasar E and Siso S H 2003 Fracture resistance of endodontically treated Premolars restored with ormocer and packable composite *J. Endodont.* **29** 838–40

[37] Al-Hiyasat A S, Darmani H and Milhem M M 2005 Cytotoxicity evaluation of dental resin composites and their flowable derivatives *Clin. Oral Investig.* **9** 21–5

[38] Popall M and Durand H 1992 Inorganic organic copolymers as solid-state Li^+ electrolytes *Electrochim. Acta* **37** 1593–7

[39] Popall M and Du X M 1995 Inorganic–organic copolymers as solid-state ionic conductors with grafted anions *Electrochim. Acta* **40** 2305–8
[40] Depre L, Kappel J and Popall M 1998 Inorganic–organic proton conductors based on alkylsulfone functionalities and their patterning by photoinduced methods *Electrochim. Acta* **43** 1301–6
[41] Depre L, Ingram M, Poinsignon C and Popall M 2000 Proton conducting sulfon/sulfonamide functionalized materials based on inorganic–organic matrices *Electrochim. Acta* **45** 1377–83
[42] Buestrich R, Kahlenberg F, Popall M, Dannberg P, Muller-Fiedler R and Rosch O 2001 ORMOCER®s for optical interconnection technology *J. Sol–Gel Sci. Technol.* **20** 181–6
[43] Popall M, Dabek A, Robertsson M E, Valizadeh S, Hagel O J, Buestrich R, Nagel R, Cergel L, Lambert D and Schaub M 2000 ORMOCER®s – inorganic–organic hybrid materials for e/o-interconnection-technology *Mol. Cryst. Liquid Cryst.* **354** 711–30
[44] Popall M, Houbertz R, Frohlich L, Streppel U, Dannberg P, Westenhofer S and Gale M 2003 ORMOCER®s – inorganic–organic hybrid materials for integrated, diffractive and refractive microoptics: synthesis, processing, and applications in optical components *Glass Sci. Technol.* **76** 53–8
[45] Serbin J, Egbert A, Ostendorf A, Chichkov B N, Houbertz R, Domann G, Schulz J, Cronauer C, Frohlich L and Popall M 2003 Femtosecond laser-induced two-photon polymerization of inorganic–organic hybrid materials for applications in photonics *Opt. Lett.* **28** 301–3
[46] Serbin J and Gu M 2006 Experimental evidence for superprism effects in three-dimensional polymer photonic crystals *Adv. Mater.* **18** 221–4
[47] Serbin J and Gu M 2006 Superprism phenomena in waveguide-coupled woodpile structures fabricated by two-photon polymerization *Opt. Express* **14** 3563–8
[48] Jia B H, Serbin J, Kim H, Lee B, Li J F and Gu M 2007 Use of two-photon polymerization for continuous gray-level encoding of diffractive optical elements *Appl. Phys. Lett.* **90** 073503
[49] Li J F, Jia B H, Zhou G Y, Bullen C, Serbin J and Gu M 2007 Spectral redistribution in spontaneous emission from quantum-dot-infiltrated 3D woodpile photonic crystals for telecommunications *Adv. Mater.* **19** 3276–80
[50] Li J F, Jia B H and Gu M 2008 Engineering stop gaps of inorganic–organic polymeric 3D woodpile photonic crystals with post-thermal treatment *Opt. Express* **16** 20073–80
[51] Woggon T, Kleiner T, Punke M and Lemmer U 2009 Nanostructuring of organic–inorganic hybrid materials for distributed feedback laser resonators by two-photon polymerization *Opt. Express* **17** 2500–7
[52] Karalekas D and Schizas C 2009 Monitoring of solidification induced strains in two resins used in photofabrication *Mater. Des.* **30** 3705–12
[53] Ovsianikov A, Ostendorf A and Chichkov B N 2007 Three-dimensional photofabrication with femtosecond lasers for applications in photonics and biomedicine *Appl. Surf. Sci.* **253** 6599–602
[54] Ovsianikov A, Chichkov B, Adunka O, Pillsbury H, Doraiswamy A and Narayan R J 2007 Rapid prototyping of ossicular replacement prostheses *Appl. Surf. Sci.* **253** 6603–7
[55] Narayan R J, Jin C M, Doraiswamy A, Mihailescu I N, Jelinek M, Ovsianikov A, Chichkov B and Chrisey D B 2005 Laser processing of advanced bioceramics *Adv. Eng. Mater.* **7** 1083–98
[56] Ovsianikov A, Chichkov B, Mente P, Monteiro-Riviere N A, Doraiswamy A and Narayan R J 2007 Two photon polymerization of polymer–ceramic hybrid materials for transdermal drug delivery *Int. J. Appl. Ceram. Technol.* **4** 22–9
[57] Doraiswamy A, Jin C, Narayan R J, Mageswaran P, Mente P, Modi R, Auyeung R, Chrisey D B, Ovsianikov A and Chichkov B 2006 Two photon induced polymerization of organic–inorganic hybrid biomaterials for microstructured medical devices *Acta Biomater.* **2** 267–75
[58] Saravanamuttu K, Blanford C F, Sharp D N, Dedman E R, Turberfield A J and Denning R G 2003 Sol–gel organic–inorganic composites for 3D holographic lithography of photonic crystals with submicron periodicity *Chem. Mater.* **15** 2301–4
[59] Segawa H, Yamaguchi S, Yamazaki Y, Yano T, Shibata S and Misawa H 2006 Top-gathering pillar array of hybrid organic–inorganic material by means of self-organization *Appl. Phys.* A **83** 447–51
[60] Que W X, Jia C Y, Sun M, Sun Z, Wang L L and Zhang Z J 2008 Photo-patternable GeO2-contained organic–inorganic hybrid sol–gel films for photonic applications *Opt. Express* **16** 3490–5
[61] Di Maggio R, Fambri L and Guerriero A 1998 Zirconium alkoxides as components of hybrid inorganic–organic macromolecular materials *Chem. Mater.* **10** 1777–84
[62] Schubert U 2003 Silica-based and transition metal-based inorganic–organic hybrid materials—a comparison *J. Sol–Gel Sci. Technol.* **26** 47–55
[63] Duan X M, Sun H B, Kaneko K and Kawata S 2004 Two-photon polymerization of metal ions doped acrylate monomers and oligomers for three-dimensional structure fabrication *Thin Solid Films* **453/454** 518–21
[64] Sun Z B, Dong X Z, Chen W Q, Shoji S, Duan X M and Kawata S 2008 Two- and three-dimensional micro/nanostructure patterning of CdS–polymer nanocomposites with a laser interference technique and *in situ* synthesis *Nanotechnology* **19** 035611
[65] Sun Z B, Dong X Z, Chen W Q, Nakanishi S, Duan X M and Kawata S 2008 Multicolor polymer nanocomposites: *in situ* synthesis and fabrication of 3D microstructures *Adv. Mater.* **20** 914–9
[66] Bhuian B, Winfield R J, O'Brien S and Crean G M 2006 Investigation of the two-photon polymerisation of a Zr-based inorganic–organic hybrid material system *Appl. Surf. Sci.* **252** 4845–9
[67] Winfield R J, Bhuian B, O'Brien S and Crean G M 2007 Refractive femtosecond laser beam shaping for two-photon polymerization *Appl. Phys. Lett.* **90** 111115
[68] Winfield R J, Bhuian B, O'Brien S and Crean G M 2007 Fabrication of grating structures by simultaneous multi-spot fs laser writing *Appl. Surf. Sci.* **253** 8086–90
[69] Ovsianikov A *et al* 2008 Ultra-low shrinkage hybrid photosensitive material for two-photon polymerization microfabrication *ACS Nano* **2** 2257–62
[70] Ovsianikov A *et al* 2008 Two-photon polymerization of hybrid sol–gel materials for photonics applications *Laser Chem.* **2008** 493059
[71] Ovsianikov A, Shizhou X, Farsari M, Vamvakaki M, Fotakis C and Chichkov B N 2009 Shrinkage of microstructures produced by two-photon polymerization of Zr-based hybrid photosensitive materials *Opt. Express* **17** 2143–8
[72] Sun Q, Juodkazis S, Murazawa N, Mizeikis V and Misawa H 2010 Freestanding and movable photonic microstructures fabricated by photopolymerization with femtosecondlaser pulses *J. Micromech. Microeng.* **20** 035004

[73] Sakellari I, Gaidukeviciute A, Giakoumaki A, Gray D, Fotakis C, Vamvakaki M, Farsari M, Reinhardt C, Ovsianikov A and Chichkov B N 2009 *Direct Laser Writing of Photonic Nanostructures* ed A N Mikhail *et al* (Bellingham, WA: SPIE Optical Engineering Press) p 73920Y
[74] Correa D S, Tayalia P, Cosendey G, dos Santos D S, Aroca R F, Mazur E and Mendonca C R 2009 Two-photon polymerization for fabricating structures containing the biopolymer chitosan *J. Nanosci. Nanotechnol.* **9** 5845–9
[75] Mendonca C R, Correa D S, Marlow F, Voss T, Tayalia P and Mazur E 2009 Three-dimensional fabrication of optically active microstructures containing an electroluminescent polymer *Appl. Phys. Lett.* **95** 113309
[76] Norwood R A *et al* 2007 Hybrid sol–gel electro-optic polymer modulators: beating the drive voltage/loss tradeoff *J. Nonlinear Opt. Phys. Mater.* **16** 217–30
[77] Goudket H, Canva M, Levy Y, Chaput F and Boilot J P 2001 Temperature dependence of second-order nonlinear relaxation of a poled chromophore-doped sol–gel material *J. Appl. Phys.* **90** 6044–7
[78] Zhang H X, Lu D, Peyghambarian N, Fallahi M, Luo J D, Chen B Q and Jen A K Y 2005 Electro-optic properties of hybrid solgel doped with a nonlinear chromophore with large hyperpolarizability *Opt. Lett.* **30** 117–9
[79] Enami Y *et al* 2007 Hybrid polymer/sol–gel waveguide modulators with exceptionally large electro-optic coefficients *Nat. Photon.* **1** 180–5
[80] Zhang H X, Lu D, Liu T, Mansuripur M and Fallahi M 2004 Direct laser writing of electro-optic waveguide in chromophore-doped hybrid sol–gel *Appl. Phys. Lett.* **85** 4275–7
[81] Lu D, Zhang H X and Fallahi M 2005 Electro-optic modulation in hybrid solgel doped with disperse red chromophore *Opt. Lett.* **30** 278–80
[82] Zhang H X and Fallahi M 2005 Electro-optic waveguide based on hybrid sol–gel doped with organic chromophore *Opt. Commun.* **248** 415–8
[83] Zhang H X, Lu D and Fallahi M 2006 Nonlinear optical and electro-optic properties of hybrid sol–gels doped with organic chromophores *Opt. Mater.* **28** 992–9
[84] Tien P K, Smolinsky G and Martin R J 1972 Thin organosilicon films for integrated optics *Appl. Opt.* **11** 637–42
[85] Monneret S, Huguet-Chantôme P and Flory F 2000 m-lines technique: prism coupling measurement and discussion of accuracy for homogeneous waveguides *J. Opt.* A **2** 188–95
[86] Riehl D, Chaput F, Levy Y, Boilot J P, Kajzar F and Chollet P A 1995 Second-order optical nonlinearities of azo chromophores covalently attached to a sol–gel matrix *Chem. Phys. Lett.* **245** 36–40
[87] Chen Y S, Tal A, Torrance D B and Kuebler S M 2006 Fabrication and characterization of three-dimensional silver-coated polymeric microstructures *Adv. Funct. Mater.* **16** 1739–44
[88] Kaneko K, Yamamoto K, Kawata S, Xia H, Song J F and Sun H B 2008 Metal-nanoshelled three-dimensional photonic lattices *Opt. Lett.* **33** 1999–2001
[89] Rill M S, Plet C, Thiel M, Staude I, Von Freymann G, Linden S and Wegener M 2008 Photonic metamaterials by direct laser writing and silver chemical vapour deposition *Nat. Mater.* **7** 543–6
[90] Drakakis T S, Papadakis G, Sambani K, Filippidis G, Georgiou S, Gizeli E, Fotakis C and Farsari M 2006 Construction of three-dimensional biomolecule structures employing femtosecond lasers *Appl. Phys. Lett.* **89** 144108
[91] Farsari M, Filippidis G, Drakakis T S, Sambani K, Georgiou S, Papadakis G, Gizeli E and Fotakis C 2007 Three-dimensional biomolecule patterning *Appl. Surf. Sci.* **253** 8115–8
[92] Rozsnyai L F, Benson D R, Fodor S P A and Schultz P G 1992 Photolithographic immobilization of biopolymers on solid supports *Angew. Chem. Int. Edn* **31** 759–61
[93] Holden M A and Cremer P S 2003 Light activated patterning of dye-labeled molecules on surfaces *J. Am. Chem. Soc.* **125** 8074–5
[94] Choi H J, Kim N H, Chung B H and Seong G H 2005 Micropatterning of biomolecules on glass surfaces modified with various functional groups using photoactivatable biotin *Anal. Biochem.* **347** 60–6
[95] Balakirev M Y, Porte S, Vernaz-Gris M, Berger M, Arie J P, Fouque B and Chatelain F 2005 Photochemical patterning of biological molecules inside a glass capillary *Anal. Chem.* **77** 5474–9
[96] Smith C L, Milea J S and Nguyen G H 2005 *Immobilisation of DNA on Chips Ii* (Berlin: Springer) pp 63–90
[97] Dinca V, Kasotakis E, Catherine J, Mourka A, Ranella A, Ovsianikov A, Chichkov B N, Farsari M, Mitraki A and Fotakis C 2008 Directed three-dimensional patterning of self-assembled peptide fibrils *Nano Lett.* **8** 538–43
[98] Baughman R H, Zakhidov A A and de Heer W A 2002 Carbon nanotubes—the route toward applications *Science* **297** 787–92
[99] Seeman N C 2003 DNA in a material world *Nature* **421** 427–31
[100] Braun E, Eichen Y, Sivan U and Ben-Yoseph G 1998 DNA-templated assembly and electrode attachment of a conducting silver wire *Nature* **391** 775–8
[101] van Raaij M J and Mitraki A 2004 Beta-structured viral fibres: assembly, structure and implications for materials design *Curr. Opin. Solid State Mater. Sci.* **8** 151–6
[102] Zhang S G 2003 Fabrication of novel biomaterials through molecular self-assembly *Nat. Biotechnol.* **21** 1171–8
[103] Gilead S and Gazit E 2005 Self-organization of short peptide fragments: from amyloid fibrils to nanoscale supramolecular assemblies *Supramol. Chem.* **17** 87–92
[104] Yemini M, Reches M, Rishpon J and Gazit E 2005 Novel electrochemical biosensing platform using self-assembled peptide nanotubes *Nano Lett.* **5** 183–6
[105] Yang H, Fung S Y, Sun W, Mikkelsen S, Pritzker M and Chen P 2008 Ionic-complementary peptide-modified highly ordered pyrolytic graphite electrode for biosensor application *Biotechnol. Prog.* **24** 964–71
[106] Cho E C, Choi J W, Lee M Y and Koo K K 2008 Fabrication of an electrochemical immunosensor with self-assembled peptide nanotubes *Colloid Surf.* A **313** 95–9
[107] Reiss B D, Mao C B, Solis D J, Ryan K S, Thomson T and Belcher A M 2004 Biological routes to metal alloy ferromagnetic nanostructures *Nano Lett.* **4** 1127–32
[108] Mao C B, Solis D J, Reiss B D, Kottmann S T, Sweeney R Y, Hayhurst A, Georgiou G, Iverson B and Belcher A M 2004 Virus-based toolkit for the directed synthesis of magnetic and semiconducting nanowires *Science* **303** 213–7
[109] Lee S W, Mao C B, Flynn C E and Belcher A M 2002 Ordering of quantum dots using genetically engineered viruses *Science* **296** 892–5
[110] Haines-Butterick L, Rajagopal K, Branco M, Salick D, Rughani R, Pilarz M, Lamm M S, Pochan D J and Schneider J P 2007 Controlling hydrogelation kinetics by peptide design for three-dimensional encapsulation and injectable delivery of cells *Proc. Natl Acad. Sci. USA* **104** 7791–6
[111] Gelain F, Horii A and Zhang S G 2007 Designer self-assembling peptide scaffolds for 3D tissue cell cultures and regenerative medicine *Macromol. Biosci.* **7** 544–51

[112] Serbin J, Ovsianikov A and Chichkov B 2004 Fabrication of woodpile structures by two-photon polymerization and investigation of their optical properties *Opt. Express* **12** 5221–8

[113] Ovsianikov A, Passinger S, Houbertz R and Chichkov B N 2006 Laser ablation and its applications *Laser Ablation and its Applications* ed C R Phipps (Berlin: Springer) pp 129–67

[114] Schizas C, Melissinaki V, Gaidukeviciute A, Reinhardt C, Ohrt C, Dedoussis V, Chichkov B N, Fotakis C, Farsari M and Karalekas D 2009 On the design and fabrication by two-photon polymerization of a readily assembled micro-valve *Int. J. Adv. Manuf. Technol.* at press doi:10.1007/s00170-009-2320-4

[115] Sakellari I, Gaidukeviciute A, Giakoumaki A, Gray D, Fotakis C, Vamvakaki M, Farsari M, Reinhardt C, Ovsianikov A and Chichkov B N 2009 Direct laser writing of photonic nanostructures *Metamaterials: Fundamentals and Applications* vol II (Bellingham, WA: SPIE Optical Engineering Press) pp 73920Y1–9

[116] Farsari M, Ovsianikov A, Vamvakaki M, Sakellari I, Gray D, Chichkov B N and Fotakis C 2008 Fabrication of three-dimensional photonic crystal structures containing an active nonlinear optical chromophore *Appl. Phys.* A **93** 11–5